OpenFOAM GUIDE FOR BEGINNERS

OpenFOAM®

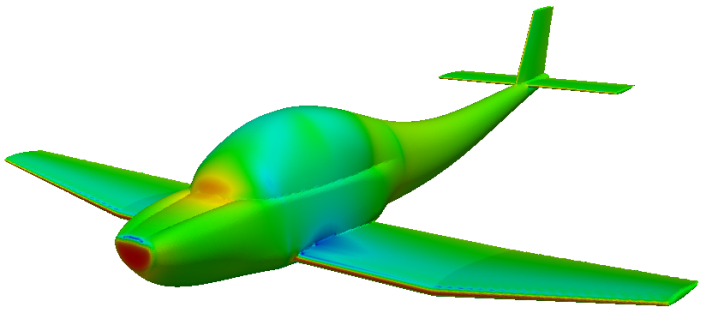

Escola Tècnica Superior d'Enginyeries
Industrial i Aeronàutica de Terrassa
UNIVERSITAT POLITÈCNICA DE CATALUNYA

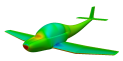

This guide has been developed by:

Jordi Casacuberta Puig

In association with:

Pedro Javier Gamez and Gustavo Raush

The Foam House ETSEIAT-UPC
Barcelona June 2014

Contents

Contents i

List of Figures v

List of Tables ix

1 Introduction 1
- 1.0.1 About *OpenFOAM*® . . . 1
- 1.0.2 About this guide . . . 1
- 1.0.3 Notes . . . 2

2 Plane-parallel plates laminar flow 3
- 2.1 Description of the case . . . 3
- 2.2 Hypotheses . . . 3
- 2.3 First case: plane-parallel plates with relative movement (Couette flow) 4
  - 2.3.1 Physics of the problem . . . 4
  - 2.3.2 Pre-processing . . . 5
    - 2.3.2.1 Mesh generation . . . 6
    - 2.3.2.2 Boundary and initial conditions . . . 14
    - 2.3.2.3 Physical properties . . . 19
    - 2.3.2.4 Control . . . 21
    - 2.3.2.5 Discretization and linear-solver settings . . . 24
    - 2.3.2.6 Creating the mesh . . . 26
  - 2.3.3 Viewing the mesh . . . 28
  - 2.3.4 Running the application . . . 29
  - 2.3.5 Post-processing . . . 30
    - 2.3.5.1 Viewing the results as isosurface and contour plots . 30
    - 2.3.5.2 Plotting variables in ParaView . . . 32
- 2.4 Second case: plane-parallel plates with pressure gradient (plane-Poiseuille flow) . . . 33
  - 2.4.1 Physics of the problem . . . 33
  - 2.4.2 Pre-processing . . . 35
    - 2.4.2.1 Boundary and initial conditions . . . 35
    - 2.4.2.2 Control . . . 38
  - 2.4.3 Post-processing . . . 39

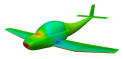

2.4.3.1 Results of the simulation . . . 39
2.5 Third case: plane-parallel plates with relative movement and pressure gradient (Couette flow with pressure gradient) . . . 42
2.5.1 Physics of the problem . . . 42
2.5.2 Pre-processing . . . 43
2.5.2.1 Boundary and initial conditions . . . 43
2.5.3 Post-processing . . . 44
2.5.3.1 Results of the simulation . . . 44
2.6 Additional utilities . . . 47
2.6.1 Vector plots . . . 47
2.6.2 Streamlines . . . 48
2.6.3 Computation of the volumetric flow rate . . . 49
2.6.3.1 Refinement of the mesh . . . 51
2.6.4 Computation of the wall shear stress . . . 55
2.6.4.1 Creation of a graded mesh . . . 58

3 Bidimensional laminar flow around a circular cylinder 61
3.1 Description of the case . . . 61
3.2 Hypotheses . . . 61
3.3 Physics of the problem . . . 61
3.4 Pre-processing with $Re = 195$ . . . 64
3.4.1 Mesh generation . . . 64
3.4.2 Boundary and initial conditions . . . 72
3.4.3 Physical properties . . . 75
3.4.4 Control . . . 76
3.4.5 Discretization and linear-solver settings . . . 77
3.5 Post-processing . . . 79
3.5.1 Results of the simulation with $Re = 195$ . . . 79
3.5.2 Comparative between cases with $Re = 30$ and $Re = 195$ . . . 85
3.6 Additional utilities . . . 87
3.6.1 Vorticity . . . 87
3.6.2 Computation of the aerodynamic coefficients . . . 88
3.6.3 Plotting the results with Gnuplot . . . 89
3.6.4 Computation of the stream function . . . 91
3.6.5 Convertion to VTK . . . 92

4 Laminar flow through a circular pipe 93
4.0.6 Description of the case . . . 93
4.0.7 Hypotheses . . . 93
4.0.8 Physics of the problem . . . 93
4.0.9 Pre-processing . . . 95
4.0.9.1 Mesh generation . . . 96

4.0.9.2 Boundary and initial conditions . . . 99
4.0.9.3 Physical properties . . . 102
4.0.9.4 Control . . . 102
4.0.9.5 Discretization and linear-solver settings . . . 103
4.0.10 Post-processing . . . 106
4.0.10.1 Results of the simulation . . . 106
4.0.11 Additional utilities . . . 111
4.0.11.1 Computation of average field values at patches . . . 111
4.0.11.2 Read field values with ParaView . . . 112
4.0.11.3 Plot the residuals of the simulation . . . 113

5 Aerodynamics of a 2D airfoil NACA 23012 116
5.0.12 Description of the case . . . 116
5.0.13 Hypotheses . . . 116
5.0.14 Physics of the problem . . . 116
5.0.15 Pre-processing with $\alpha = 15^o$ . . . 119
5.0.15.1 Mesh generation . . . 119
5.0.15.2 Boundary and initial conditions . . . 123
5.0.15.3 Physical properties . . . 128
5.0.15.4 Control . . . 129
5.0.15.5 Discretization and linear-solver settings . . . 130
5.0.16 Post-processing . . . 134
5.0.16.1 Results of the simulation for $\alpha = 15^o$ . . . 134
5.0.16.2 Results of the simulation for a range of α. Plot of the main aerodynamic curves . . . 137
5.0.17 Additional utilities . . . 140
5.0.17.1 Mesh conversion . . . 140
5.0.17.2 Computation of y^+ . . . 141
5.0.17.3 Isobars around a body . . . 143
5.0.17.4 Tube-like streamlines . . . 143

6 Fluid dynamics of a Very Light Aircraft 145
6.0.18 Description of the case . . . 145
6.0.19 Hypotheses . . . 145
6.0.20 Physics of the problem . . . 146
6.0.21 Pre-processing . . . 149
6.0.21.1 Mesh generation . . . 149
6.0.21.2 Boundary and initial conditions . . . 167
6.0.21.3 Physical properties . . . 173
6.0.21.4 Control . . . 174
6.0.21.5 Discretization and linear-solver settings . . . 175
6.0.21.6 External functions . . . 178

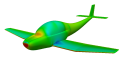

6.0.22 Post-processing 181
6.0.22.1 Results of the simulation 181

A Additional codes **184**

Bibliography **193**

List of Figures

1.1 Overview of OpenFOAM structure, extracted from [1] 1

2.1 Viscous incompressible flow between two plane-parallel plates with relative movement 4
2.2 Domain of the *Couette flow* case 6
2.3 Specifications of a single block 11
2.4 Mesh grading along a block edge 11
2.5 Patches defined in the domain of ppWall 13
2.6 Initial mesh of the ppWall case 14
2.7 Base units and nomenclature for SI and USCS, extracted from [1] . . 16
2.8 ParaView's window with the initial ppWall mesh 28
2.9 Velocity field obtained with icoFoam in the *Couette flow* case (m/s) . 31
2.10 Pressure field obtained with icoFoam in the *Couette flow* case (m^2/s^2) 32
2.11 Distribution of $|\mathbf{U}|$ and p (ordinate axis) along the y-axis (abscissa axis) obtained with the icoFoam simulation of the *Couette flow* case 33
2.12 Viscous incompressible flow between two plane-parallel plates with a pressure gradient in the x-direction 34
2.13 Velocity field obtained with icoFoam in the *plane-Poiseuille flow* case (m/s) 40
2.14 Pressure field obtained with icoFoam in the *plane-Poiseuille flow* case (m^2/s^2) 40
2.15 Distribution of $|\mathbf{U}|$ (ordinate axis) along the y-axis (abscissa axis) obtained with the icoFoam simulation of the *plane-Poiseuille flow* case 41
2.16 Distribution of p (ordinate axis) along the x-axis (abscissa axis) obtained with the icoFoam simulation of the *plane-Poiseuille flow* case 41
2.17 Viscous incompressible flow between two plane-parallel plates with relative movement and with a pressure gradient in the x-direction . . 42
2.18 Velocity field obtained with icoFoam in the *Couette flow with pressure gradient* case (m/s) 45
2.19 Pressure field obtained with icoFoam in the *Couette flow with pressure gradient* case (m^2/s^2) 45
2.20 Distribution of $|\mathbf{U}|$ (ordinate axis) along the y-axis (abscissa axis) obtained with the icoFoam simulation of the *Couette flow with pressure gradient* case 46
2.21 Distribution of p (ordinate axis) along the x-axis (abscissa axis) obtained with the icoFoam simulation of the *Couette flow with pressure gradient* case 46

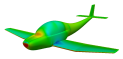

2.22 Vectors of the flow velocity in the *plane-Poiseuille flow* case (m/s) . 48
2.23 Streamlines in the *plane-Poiseuille flow* case (m/s) 49
2.24 Table containing the definition of *phi* depending whether the case is compressible or incompressible [1] 50
2.25 Shear stress at the walls of the *plane-Poiseuille flow* case (m^2/s^2) . . 57
2.26 Graded mesh used to obtain more accurate values of the wall shear stress in the *plane-Poiseuille flow* case 60

3.1 Flow around a circular cylinder 62
3.2 Flow structure depending on the Reynolds number, extracted from [2] 63
3.3 Drag coefficient as a function of the Reynolds number in an infinite circular cylinder 64
3.4 Half of the scheme used for the creation of the mesh, extracted from [1] 65
3.5 Mesh of the *bidimensional cylinder* case 71
3.6 Detail of the mesh of the *bidimensional cylinder* case 71
3.7 Detail of the mesh gradation on the walls of the *bidimensional cylinder* case 72
3.8 Velocity field around the bidimensional cylinder at $t = 0.01$ s (m/s) . 80
3.9 Velocity field around the bidimensional cylinder at $t = 0.6$ s (m/s) . 80
3.10 Velocity field around the bidimensional cylinder at $t = 1.13$ s (m/s) . 81
3.11 Pressure field around the bidimensional cylinder at $t = 0.01$ s (m^2/s^2) 81
3.12 Pressure field around the bidimensional cylinder at $t = 0.6$ s (m^2/s^2) 82
3.13 Pressure field around the bidimensional cylinder at $t = 1.13$ s (m^2/s^2) 82
3.14 Streamlines around the bidimensional cylinder at $t = 0.01$ s (m/s) . 83
3.15 Streamlines around the bidimensional cylinder at $t = 0.4$ s (m/s) . . 83
3.16 Streamlines around the bidimensional cylinder at $t = 0.6$ s (m/s) . . 84
3.17 Streamlines around the bidimensional cylinder at $t = 1.13$ s (m/s) . 84
3.18 Velocity vectors around the bidimensional cylinder at $t = 1.13$ s (m/s) 85
3.19 Vorticity field around the bidimensional cylinder at $t = 1.75$ s 87
3.20 Drag coefficient (ordinate axis) of the bidimensional cylinder at $Re = 195$ in front of time (abscissa axis) 90
3.21 Lift coefficient (ordinate axis) of the bidimensional cylinder at $Re = 195$ in front of time (abscissa axis) 90
3.22 Stream function of the velocity of the *bidimensional cylinder* case for $Re = 195$ at $t = 1.75$ s 91

4.1 Flow through a circular pipe with a constant inlet velocity 94
4.2 Scheme of the domain of the circularPipe case, extracted from [1] . . 96
4.3 Initial mesh of the circularPipe case 98
4.4 Velocity field at the inlet of the pipe in the circularPipe case (m/s) . 107
4.5 Velocity field at the outlet of the pipe in the circularPipe case (m/s) . 107

4.6 Pressure field in the circularPipe case (m^2/s^2) . . . 108
4.7 Streamlines of the flow at the inlet of the pipe in the circularPipe case (m/s) . . . 108
4.8 Streamlines of the flow at the outlet of the pipe in the circularPipe case (m/s) . . . 109
4.9 Plot of $|\mathbf{U}|$ (ordinate axis) as a function of r (abscissa axis) at the outlet of the pipe in the circularPipe case . . . 109
4.10 Plot of p (ordinate axis) as a function of z (abscissa axis) in the circularPipe case . . . 110
4.11 Plot of τ_w (ordinate axis) as a function of z (abscissa axis) in the circularPipe case . . . 111
4.12 Menu to read field data in ParaView . . . 113
4.13 Residuals of the velocity in the circularPipe case . . . 115
4.14 Residuals of the pressure in the circularPipe case . . . 115

5.1 Airfoil NACA 23012 flying at 45 m/s and ambient pressure . . . 117
5.2 NACA 23012 . . . 118
5.3 Global view of the mesh of the alpha15 case . . . 122
5.4 Airfoil shape in the mesh of the alpha15 case . . . 122
5.5 Detail of the mesh grading at the walls of the alpha15 case . . . 123
5.6 Velocity field around the NACA 23012 at $\alpha = 15^o$ (m/s) . . . 134
5.7 Pressure field around the NACA 23012 at $\alpha = 15^o$ (m^2/s^2) . . . 135
5.8 Streamlines around the NACA 23012 at $\alpha = 15^o$ (m/s) . . . 135
5.9 Velocity vectors around the NACA 23012 at $\alpha = 15^o$ (m/s) . . . 136
5.10 Distribution of $\tilde{\nu}_t$ in the domain of the alpha15 case . . . 136
5.11 Evolution of the lift coefficient (ordinate axis) with the time (abscissa axis) in the alpha15 case . . . 137
5.12 Behaviour of the flow around the NACA 23012 at $\alpha = 0^o$ (m/s) . . . 138
5.13 Behaviour of the flow around the NACA 23012 at $\alpha = 10^o$ (m/s) . . . 138
5.14 Behaviour of the flow around the NACA 23012 at $\alpha = 20^o$ (m/s) . . . 139
5.15 Relation between C_l (ordinate axis) and α (abscissa axis) for the NACA 23012 . . . 139
5.16 Relation between C_l (ordinate axis) and C_d (abscissa axis), polar curve, for the NACA 23012 . . . 140
5.17 Distribution of y^+ at the wall of the airfoil in the alpha15 case at $t = 10000$ s . . . 142
5.18 Isobars around the NACA 23012 at the alpha15 case at $t = 10000$ s (m^2/s^2) . . . 143
5.19 Streamlines around the NACA 23012 at the alpha15 case at $t = 10000$ s (m/s) . . . 144
5.20 Tube-like streamlines around the NACA 23012 at the alpha15 case at $t = 10000$ s (m/s) . . . 144

6.1 Aircraft used in the simulation of the *Very Light Aircraft* case . . . 146

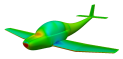

6.2 Measures of the aircraft used in the simulation of the *Very Light Aircraft* case . . . 147
6.3 Very light aircraft flying at 45 m/s and ambient pressure . . . 147
6.4 Aircraft' STL surface used in the simulation of the *Very Light Aircraft* case . . . 151
6.5 Aircraft' STL surface contained within the mesh generated with blockMesh in the *Very Light Aircraft* case . . . 154
6.6 Shape of the aircraft at the first step of the meshing process of snappyHexMesh . . . 163
6.7 Mesh of the domain at the first step of the meshing process of snappyHexMesh . . . 164
6.8 Detail of the mesh at the first step of the meshing process of snappyHexMesh . . . 164
6.9 Detail of the mesh with a representation of the cell refinement at the first step of the meshing process of snappyHexMesh . . . 165
6.10 Pressure field around the aircraft (m^2/s^2) . . . 182
6.11 Velocity field in the domain of the aircraft case (m/s) . . . 182
6.12 Velocity field around the aircraft (m/s) . . . 183

List of Tables

1. Introduction

1.0.1 About *OpenFOAM*®

OpenFOAM is first and foremost a *C++ library*, used primarily to create executables, known as *applications*. The applications fall into two categories: *solvers*, that are each designed to solve a specific problem in continuum mechanics; and *utilities*, that are designed to perform tasks that involve data manipulation. The OpenFOAM distribution contains numerous solvers and utilities covering a wide range of problems.

One of the strengths of OpenFOAM is that new solvers and utilities can be created by its users with some pre-requisite knowledge of the underlying method, physics and programming techniques involved.

OpenFOAM is supplied with pre- and post-processing environments. The interface to the pre- and post- processing are themselves OpenFOAM utilities, thereby ensuring consistent data handling across all environments. The overall structure of OpenFOAM is shown in Figure 1.1 [1]:

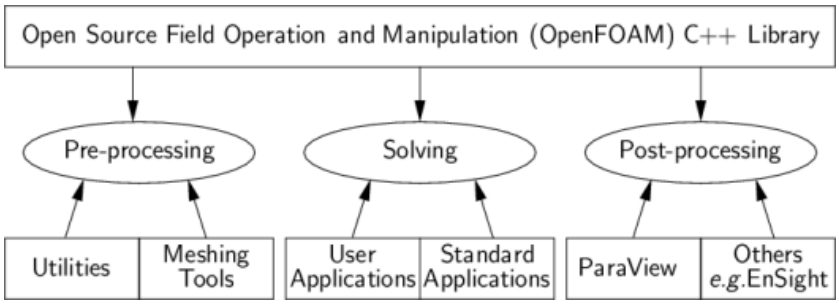

Figure 1.1: Overview of OpenFOAM structure, extracted from [1]

1.0.2 About this guide

The OpenFOAM guide developed in this project allows new users to establish and extend their OpenFOAM background once the main tutorial of the official guide is

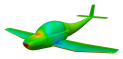

done. Then with the present guide it will be possible to improve comprehension of the OpenFOAM structure, learn programming techniques, understand how to mesh different kinds of geometries (2D and 3D), acquire familiarity with the main pre- and post-processing OpenFOAM and ParaView capabilities, figure out which solvers and physical models are more adequate for each kind of fluid mechanics problem, and much more. It should then be much easier to use complex utilities found in Internet and follow specific tutorials focused on advanced tools.

The current guide studies and exposes five different types of solved fluid mechanics problems with high applicability potential and all of them included in the same document. It has been designed to guide the user throughout the cases, starting by simple ones and following an increasing degree of difficulty. The guide offers theoretical background before developing each case, includes OpenFOAM codes needed for the simulations, gives explanations of the main physical models required for the resolution of each case, incorporates advice against typical pitfalls, and shows different and relevant OpenFOAM utilities in each chapter.

This product is not approved or endorsed by ESI Group. There is no attempt to profit from this guide; it only aims to assist new users and facilitate learning of the main OpenFOAM characteristics.

This guide is given fully for free. The author will not be responsible for any harm of any kind that these codes and their uses may cause. Readers may use the codes under their own responsibility and risk.

Send feedback to casacuberta.puig@gmail.com if you wish. I hope you find it useful.

1.0.3 Notes

In this project, Version 2.2.1 of OpenFOAM has been used.

All the plots are in SI units, except for the airfoil and the aircraft cases, where the angle α of attack is expressed in degrees.